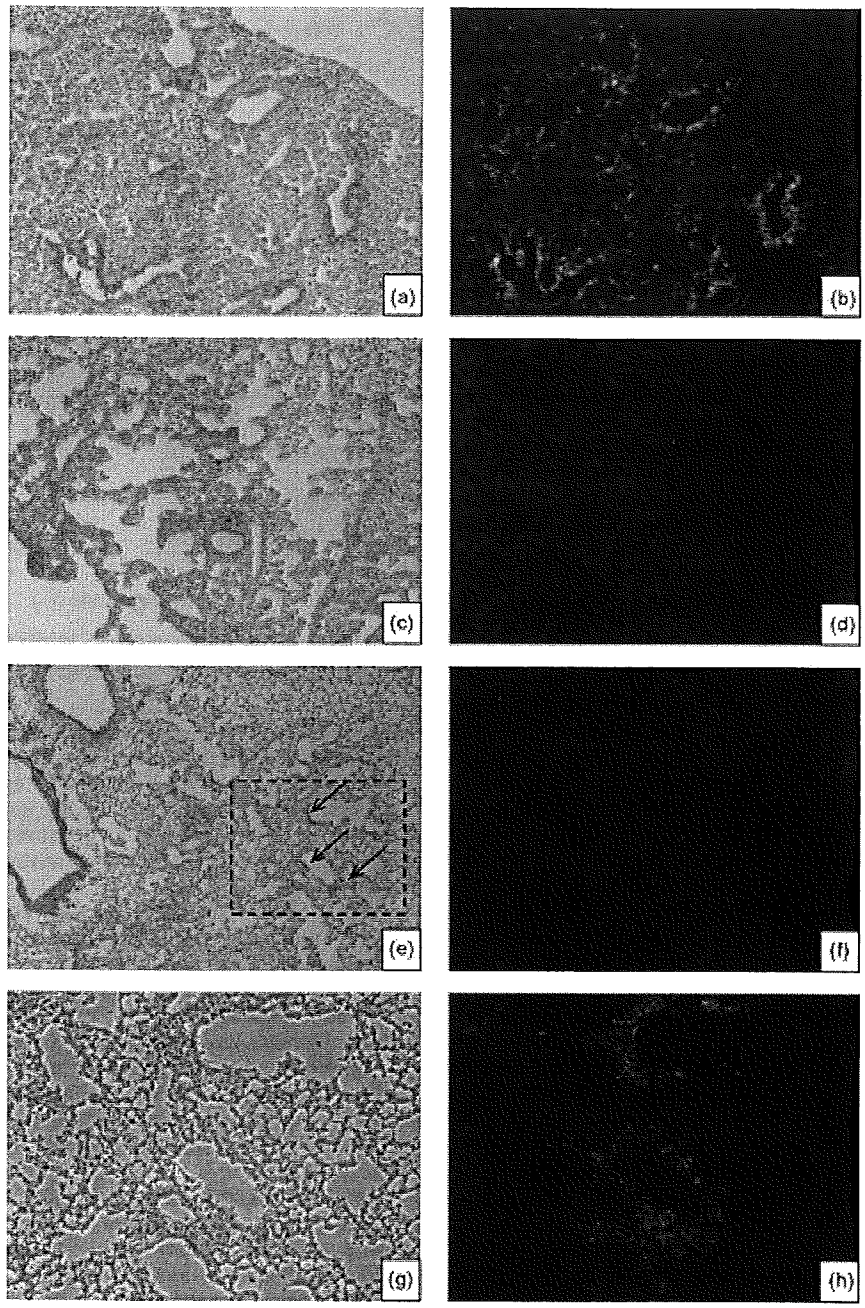

Fig. 7. Distribution of rhodamine-labeled MHAPC lipoplexes (a–d; before immunohistochemistry) and luciferase location in the lungs (e–h; after immunohistochemistry). a–f are shown at 40× magnification; g and h show 100× magnification of the regions in the dashed squares in e and f. Arrows in e indicate the luciferase (dark brown colored).

4. Conclusions

In the present work, three CCDs with a carbamate ester linker and a hydroxyethyl group were synthesized and formulated into liposomes and nanoparticles. In *in vitro* formulations, liposomes formulated with CCDs and DOPE of 1/2 molar ratio were more effective than the corresponding nanoparticles with CCDs and Tween 80 at all charge ratios. Furthermore, among the liposomal formulations, non-hydroxyethylated CCDs such as DC-Chol and DMAPC were more effective than hydroxyethylated ones in A549 cells. Gene transfection in the lung showed opposite results to those *in vitro*, with liposomes containing hydroxyethylated CCDs being more potent than ones containing non-hydroxyethylated CCDS. MHAPC liposomes, which contained a hydroxyethylated tertiary amine as the cationic part, showed the highest gene expression among CCD liposomes. All the lipoplexes caused higher TNF-α levels in the lung than the nanoplexes and jet-PEI and we considered the toxicity was largely caused by the lipoplex formulation, but our findings demonstrated that use of CCD lipoplexes with modification of the cationic cholesterol with a hydroxyethyl group at the tertiary amine headgroup, MHAPC, promoted gene expression in the lung without increasing the toxicity compared to other CCD lipoplexes. However, further efforts should be made to elucidate the mechanism of toxicity in the lung caused by CCD lipoplex and how to minimize the inflammation response of CCD lipoplex by optimizing the formulation.

Acknowledgements

This work was supported by a research grant of fiscal year 2006 from The Nagai Foundation, Tokyo and partially supported by the Ministry of Education, Culture, Sports, Sciences and Technology, Japan, and by the Open Research Center Project.

References

Arpicco, S., Canevari, S., Ceruti, M., Galmozzi, E., Rocco, F., Cattel, L., 2004. Synthesis, characterization and transfection activity of new saturated and unsaturated cationic lipids. Farmaco 59, 869–878.

Bajaj, A., Kondiah, P., Bhattacharya, S., 2007. Design, synthesis, and in vitro gene delivery efficacies of novel cholesterol-based Gemini cationic lipids and their serum compatibility: a structure–activity investigation. J. Med. Chem. 50, 2432–2442.

Choi, J.S., Lee, E.J., Jang, H.S., Park, J.S., 2001. New cationic liposomes for gene transfer into mammalian cells with high efficiency and low toxicity. Bioconjug. Chem. 12, 108–113.

Driscoll, K.E., Costa, D.L., Hatch, G., Henderson, R., Oberdorster, G., Salem, H., Schlesinger, R.B., 2000. Intratracheal instillation as an exposure technique for the evaluation of respiratory tract toxicity: uses and limitations. Toxicol. Sci. 55, 24–35.

Gao, X., Huang, L., 1991. A. novel cationic liposome reagent for efficient transfection of mammalian cells. Biochem. Biophys. Res. Commun. 179, 280–285.

Ghosh, Y.K., Visweswariah, S.S., Bhattacharya, S., 2002. Advantage of the ether linkage between the positive charge and the cholesteryl skeleton in cholesterol-based amphiphiles as vectors for gene delivery. Bioconjug. Chem. 13, 378–384.

Hasegawa, S., Hirashima, N., Nakanishi, M., 2002. Comparative study of transfection efficiency of cationic cholesterols mediated by liposomes-based gene delivery. Bioorg. Med. Chem. Lett. 12, 1299–1302.

Hattori, Y., Kubo, H., Higashiyama, K., Maitani, Y., 2005. Folate-linked nanoparticles formed with DNA complexes in sodium chloride solution enhance transfection efficiency. J. Biomed. Nanotechnol. 1, 176–184.

Hattori, Y., Ding, W., Maitani, Y., 2007. Highly efficient cationic hydroxyethylated cholesterol-based nanoparticle-mediated gene transfer in vivo and in vitro in prostate carcinoma PC-3 cells. J. Control. 120, 122–132.

Hong, H., 2005. Gene therapy rising? Nature 435, 530–531.

Igarashi, S., Hattori, Y., Maitani, Y., 2006. Biosurfactant MEL-A enhances cellular association and gene transfection by cationic liposome. J. Control. Release 112, 362–368.

Lee, E.J., Lee, M., Park, J.S., Choi, J.S., 2006. Synthesis of 3β [L-lysinamide-carbamoyl] cholesterol derivatives by solid-phase method and characteristics of complexes with antisense oligodeoxynucleotides. Bull. Korean Chem. Soc. 27, 1020–1024.

Maitani, Y., Igarashi, S., Sato, M., Hattori, Y., 2007. Cationic liposome (DC-Chol/DOPE = 1:2) and a modified ethanol injection method to prepare liposomes, increased gene expression. Int. J. Pharm..

Miller, A.D., 2003. The problem with cationic liposome/micelle-based non-viral vector systems for gene therapy. Curr. Med. Chem. 10, 1195–1211.

Nakanishi, M., 2003. New strategy in gene transfection by cationic transfection lipids with a cationic cholesterol. Curr. Med. Chem. 10, 1289–1296.

Nakanishi, M., Noguchi, A., 2001. Confocal and probe microscopy to study gene transfection mediated by cationic liposomes with a cationic cholesterol derivative. Adv. Drug Deliv. Rev. 52, 197–207.

Okayama, R., Noji, M., Nakanishi, M., 1997. Cationic cholesterol with a hydroxyethylamino head group promotes significantly liposome-mediated gene transfection. FEBS Lett. 408, 232–234.

Percot, A., Briane, D., Coudert, R., Reynier, P., Bouchemal, N., Lievre, N., Hantz, E., Salzmann, J.L., Cao, A., 2004. A hydroxyethylated cholesterol-based cationic lipid for DNA delivery: effect of conditioning. Int. J. Pharm. 278, 143–163.

Pietersz, G.A., Tang, C.K., Apostolopoulos, V., 2006. Structure and design of polycationic carriers for gene delivery. Mini Rev. Med. Chem. 6, 1285–1298.

Reynier, P., Briane, D., Coudert, R., Fadda, G., Bouchemal, N., Bissieres, P., Taillandier, E., Cao, A., 2004. Modifications in the head group and in the spacer of cholesterol-based cationic lipids promote transfection in melanoma B16–F10 cells and tumours. J. Drug Target. 12, 25–38.

Rosenecker, J., Naundorf, S., Gersting, S.W., Hauck, R.W., Gessner, A., Nicklaus, P., Müller, R.H., Rudolph, C., 2003. Interaction of bronchoalveolar lavage fluid with polyplexes and lipoplexes: analysing the role of proteins and glycoproteins. J. Gene Med. 5, 49–60.

Scheule, R.K., St George, J.A., Bagley, R.G., Marshall, J., Kaplan, J.M., Akita, G.Y., Wang, K.X., Lee, E.R., Harris, D.J., Jiang, C., Yew, N.S., Smith, A.E., Cheng, S.H., 1997. Basis of pulmonary toxicity associated with cationic lipid-mediated gene transfer to the mammalian lung. Hum. Gene Ther. 8, 689–707.

Venkata Srilakshmi, G., Sen, J., Chaudhuri, A., Ramadas, Y., Madhusudhana Rao, N., 2002. Anchor-dependent lipofection with non-glycerol based cytofectins containing single 2-hydroxyethyl head groups. Biochim. Biophys. Acta 1559, 87–95.

Journal of
Nanoscience and Nanotechnology
Vol. 8, 1–8, 2008

Decaarginine-PEG-Artificial Lipid/DNA Complex for Gene Delivery: Nanostructure and Transfection Efficiency

Masahiko Furuhata[1], Radostin Danev[2], Kuniaki Nagayama[2], Yoshifumi Yamada[3], Hiroko Kawakami[4], Kazunori Toma[4], Yoshiyuki Hattori[1], and Yoshie Maitani[1,*]

[1] *Institute of Medicinal Chemistry, Hoshi University, Shinagawa-ku, Tokyo 142-8501, Japan*
[2] *National Institutes of Natural Sciences, Okazaki-shi, Aichi 444-8787, Japan*
[3] *Life Science Group, Olympus Corporation, Hachioji-shi, Tokyo 192-8512, Japan*
[4] *The Noguchi Institute, Itabashi-ku, Tokyo 173-0003, Japan*

Oligoarginine conjugates are highly efficient vectors for the delivery of plasmid DNA into cells. Decaarginine-conjugated lipid (Arg10-PEG-lipid) was synthesized and the effects of Arg10-PEG-lipid concentration at a fixed DNA concentration on transfection efficiency and the structure of the complexes were studied below and above critical micelle concentration (CMC), and at the lipid nitrogen/DNA phosphate (N/P) ratio corresponding to transfection, respectively. Arg10-PEG-lipid at the concentration below CMC showed stronger interaction with DNA by fluorescence intensity distribution analysis, and significantly higher luciferase and green fluorescent protein expression than that above CMC. A phase-contrast cryo-transmission electron microscope (cryo-TEM) experiment showed that the morphology of the complexes depended on the N/P ratio. At a low N/P ratio corresponding to that in transfection at a lipid concentration below CMC, a net-like structure developed in which plasmid DNA was involved. A further increase in the N/P ratio, a large fibrous nanostructure of complexes, was also observed. Without DNA, these structures were not obtained. The cellular uptake mechanism of complexes using flow cytometry with inhibitors suggested that complexes with two different morphologies showed similar cellular uptake and uptake mechanism, macropinocytosis. Differences in transfection efficiency of the complexes may be explained by a large fibrous nanostructure inhibiting the cellular internalization of complexes or the release of DNA from macropinosomes into cytoplasm. Arg10-PEG-lipid/DNA complexes formed a favorable nanostructure for gene delivery, depending on the N/P ratio in water.

Keywords: Decaarginine, Cell-Penetrating Peptide, Macropinocyotosis, Gene Delivery, Supramolecular Structure.

RESEARCH ARTICLE

1. INTRODUCTION

The development of a gene delivery vector is believed to be a key to the success of gene therapy. Gene delivery vectors are classified into viral and nonviral vectors. Viral vectors provide very high transfection efficiency, but their safety is a great concern because of their immunogenicity and acute toxicity.[1,2] For the future development of gene therapy, a safe and highly effective nonviral gene vector is indispensable, and nonviral vectors such as cationic liposomes and polymers have been developed;[1,3,4] however, their low-level transfection efficiency, compared with viral vectors, is considered to be a major limitation in their application to gene therapy. Poor efficiency is supposed to arise from the endocytic route of internalization, when cationic lipids or polymers form a complex with DNA; therefore, novel and more efficient synthetic vectors, hopefully with a different cell internalization mechanism, are desired.

Oligoarginine is known as a cell-penetrating peptide (CPP),[5–7] and can deliver its associated molecules into cells.[8–11] In our previous work, we reported oligoarginine ((Arg)n; $n = 4, 6, 8, 10$)-conjugated lipids with a poly(ethylene glycol) (PEG) spacer as novel gene vectors.[12] (Arg)n-PEG-lipid provides three characteristic functions: the PEG-lipid part forms micelles, the (Arg)n part can interact with DNA and make it compact, and this part

*Author to whom correspondence should be addressed.

also interacts with cells as CPP. Arg10-PEG-lipid showed the highest transfection efficiency among (Arg)*n*-PEG-lipids in human cervical carcinoma HeLa cells when the lipid formed a complex with plasmid DNA at concentrations much higher than their critical micelle concentration (CMC) to ensure the integrity of micelles.[12] Transfection efficiency was comparable to Lipofectamine 2000, a commercial transfection reagent.[12]

Cationic lipids form small particles when they form a complex with DNA molecules, which is an ideal property for efficient internalization of the complexes by endocytosis.[13] A variety of structural models have been proposed based upon electron microscopy studies about cationic liposome complexes with DNA by using a nature of helper lipids. The superior transfection properties of lipoplexes were related to its ability to undergo a lamellar to a nonlamellar phase.[14] About micelles, however, information of morphologies of complexes depending charge ratios of lipid/DNA was poor.[15] Below CMC, the relationship between transfection efficiency and structure of lipid complexes with DNA were not reported to our knowledge.

The purpose of this study was to investigate the relationship of the concentration of Arg10-PEG-lipid to lipid-mediated gene delivery. The interaction between Arg10-PEG-lipid and plasmid DNA was measured by fluorescence intensity distribution analysis (FIDA), and the morphology of Arg10-PEG-lipid/DNA complex was observed by phase contrast cryo-transmission electron microscopy (phase contrast cryo-TEM). Here, we report novel aspects of Arg10-PEG-lipid, i.e., the concentration-dependent transfection efficiency and relationship with nanostructure formation that may cause difference in the ability to deliver DNA into HeLa cells. The lipid showed higher transfection at a concentration below CMC than above CMC.

2. MATERIALS AND METHODS

2.1. Materials

The Pica gene luciferase assay kit was purchased from Toyo Ink (Tokyo, Japan). Bicinchonic acid (BCA) protein assay reagent was obtained from Pierce (Rockford, IL). Dulbecco's modified Eagle's medium (DMEM) and fetal bovine serum (FBS) were purchased from Invitrogen Corp. (Carlsbad, CA). 5-(*N*-ethyl-*N*-isopropyl) amiloride (EIPA) was from Sigma Chemical Co. (St. Louis, MO). All other chemicals used were of reagent grade.

Arg10-PEG-lipid (Arg10-PEG-BDB, Fig. 1) and 7-nitrobenz-2-oxa-1,3-diazole (NBD)-labeled Arg10-PEG-BDB (Arg10-PEG-BDB-NBD) were synthesized as described previously.[12] 3,5-Bis(dodecyloxy)benzamide (BDB) was employed as the lipid component, and a PEG (MW = 2 kDa) spacer was introduced between the C-terminal of Arg10 and the amide group of BDB.

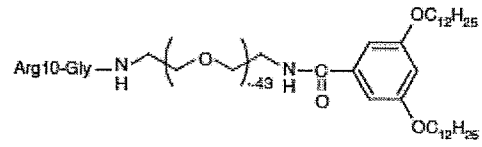

Fig. 1. Chemical structure of Arg10-PEG-BDB.

The plasmid DNA encoding the luciferase gene under the control of the CMV promoter (pCMV-luc) was constructed as previously described.[16] The plasmid pEGFP-C1 encoding the green fluorescent protein (GFP) under the CMV promoter was purchased from Clontech (Palo Alto, CA). A protein-free preparation of pCMV-luc and pEGFP-C1 was purified following alkaline lysis using maxiprep columns (Qiagen, Hilden, Germany). Labeling of pCMV-luc was performed using the protocol of a Label IT TM-rhodamine labeling kit (Mirus, Madison, WI).

2.2. Critical Micelle Concentration of Arg10-PEG-BDB

In order to determine the critical micelle concentration (CMC) of Arg10-PEG-BDB, fluorescence measurements were carried out using pyrene (0.6 μM) as reported in the literature.[17] The fluorescence emission spectra of pyrene were measured at varying Arg10-PEG-BDB concentrations using a fluorescence spectrometer. The concentration of Arg10-PEG-BDB used was within the range from 1×10^{-8} to 1×10^{-3} M. Pyrene was dissolved in acetone and transferred into capped tubes. The acetone as solvent was evaporated off by a stream of dry nitrogen, and subsequently, aqueous solutions of Arg10-PEG-BDB micelles were added. Then, the micellar solutions containing pyrene were heated to 80 °C for 2 h to equilibrate the partitioning of pyrene into the micelles and were allowed to cool over night at room temperature in the dark.

2.3. Formulation of Arg10-PEG-BDB/DNA Complex

Arg10-PEG-BDB stock solutions (20 mg/mL) were prepared by dissolving lipid in MilliQ water. Arg10-PEG-BDB/DNA complexes were formulated by mixing DNA and Arg10-PEG-BDB stock solutions. The number of nitrogen of Arg10-PEG-BDB was defined as 10 and the lipid nitrogen/DNA phosphate (N/P) ratio was calculated. For transfection and FIDA experiments, the following amounts of the Arg10-PEG-BDB to 2 μg of DNA were used to prepare Arg10-PEG-BDB/DNA complexes at various N/P ratios, e.g., N/P = 8.5; 20 μg/mL (5 μM). For transmission electron microscopy experiment, 0.25 mM of Arg10-PEG-BDB/DNA (N/P = 8.5/1) and 1.25 mM of Arg10-PEG-BDB/DNA (N/P = 42.5/1) were used, since higher Arg10-PEG-BDB concentrations are needed for observation.

Particle size and zeta potential of Arg10-PEG-BDB and its DNA complexes were measured 10–15 min after the complex had formed, using dynamic light scattering and electrophoresis method, respectively (ELS-800, Otsuka Electronics Co. Ltd, Osaka, Japan) at 25 °C after the dispersion was diluted to an appropriate volume with water.

2.4. Fluorescence Intensity Distribution Analysis (FIDA)

FIDA was performed with a MF20 microplate reader (Olympus Corp. Tokyo, Japan) using the onboard 543-nm laser at a power of 300 μW for excitation. Experiments were performed in 384-well glass-bottom plates using a sample volume of 50 μL. The FIDA data was analyzed with the MF20 software package. All single-molecule FIDAs were performed under identical conditions with respect to incubation (10 min) at room temperature. The interaction between Arg10-PEG-BDB and DNA experiments were performed using the rhodamine-labeled DNA. The concentration of the labeled DNA was held constant whereas the concentration of Arg10-PEG-BDB was varied in water.

2.5. Phase Contrast Cryo-TEM and Microscopy

Specimens for electron microscopy were prepared on Quantifoil® R1.2/1.3 holed carbon grids at a Leica EM CPC cryo-preparation station. Cryo-electron microscopy was performed on a JEOL JEM-3100FFC TEM equipped with a field emission gun (FEG), helium temperature specimen stage, omega-type energy filter and Gatan Mega-Scan 795 2 K × 2 K CCD camera. For improved contrast of ice-embedded specimens, we employed a novel Zernike-type phase plate at the back focal plane of the objective lens.[18,19] It provides a true phase contrast regime revealing details in the image that are hidden in the conventional defocus phase contrast mode. All images were taken by the CCD camera with the TEM operated at 300 kV acceleration voltage, zero-loss energy filter mode, ×60,000 indicated magnification and employing the phase plate. At that magnification, the specimen resolution at the CCD is 3.0 Å/pix. To minimize electron beam damage, we employed a minimum dose protocol which irradiates the area of interest only during image exposure. The total dose to the specimen was about 6 $e^-/Å^2$.

Arg10-PEG-BDB/DNA complexes were diluted with serum-free DMEM to 1 mL. Incubation with HeLa cells was conducted for 1 h in the absence of serum, and then the cells were washed 5 times with 1 mL of PBS. Unfixed cells were observed with an ECLIPSE TS100/100-F for Epi-fluorescence Observations (Nicon, Tokyo, Japan). The level of contrast and the brightness of the images were adjusted.

2.6. Flow Cytometry

HeLa cells were kindly provided by Toyobo Co., Ltd. (Osaka, Japan). HeLa cells were grown in DMEM supplemented with 10% FBS at 37 °C in a humidified 5% CO_2 atmosphere.

HeLa cells were grown to just before confluence in a 12-well plate. For cellular uptake, Arg10-PEG-BDB/rhodamine-DNA was diluted with DMEM containing 10% FBS to 1 mL. Incubation with HeLa cells was conducted for 3 h in the presence of serum since the cells could not be detached from the wells after incubation in the absence of serum. For inhibition of uptake, cells were preincubated for 30 min at 37 °C with DMEM containing 10% FBS in the presence of EIPA (50 μM). Subsequent incubation of the Arg10-PEG-BDB-NBD/DNA was carried out for 1 h in the presence of EIPA.

At the end of the incubation, the dishes were washed 3 times with 1 mL of PBS, and the cells were detached with 0.05% trypsin and EDTA solution. The cells were centrifuged at 1500 rpm, and the supernatant was discarded. The cells were resuspended with PBS containing 0.1% BSA and 1 mM EDTA, and directly introduced to a FACSCalibur flow cytometer (Becton Dickinson, San Jose, CA) equipped with a 488 nm argon ion laser. Data for 10000 fluorescent events were obtained by recording forward scatter (FSC) and side scatter (SSC) with green (for NBD; 530/30 nm) and red (for rhodamine; 585/42 nm) fluorescences.

2.7. Gene Transfection

Arg10-PEG-BDB/DNA complexes, prepared by mixing 2 μg of pCMV-luc or pEGFP-C1 with various concentrations of Arg10-PEG-BDB, were diluted with serum-free DMEM to 1 mL.[12] Incubation with HeLa cells was conducted for 3 h in the absence of serum, and cells were cultured for another 21 h in the presence of serum.

Luciferase expression was measured according to the instructions accompanying the luciferase assay system. Incubation was terminated by washing the plates three times with cold phosphate-buffered saline (pH 7.4) (PBS). Cell lysis solution (Pica gene) was added to the cell monolayers and subjected to freezing at −80 °C and thawing at 37 °C, followed by centrifugation at 15000 rpm for 5 s. The supernatants were frozen and stored at −80 °C until the assays. Aliquots of 20 μL of the supernatants were mixed with 100 μL of luciferin solution (Pica gene) and counts per second (cps) were measured with a chemoluminometer (Wallac ARVO SX 1420 multilabel counter, Perkin-Elmer Life Science, Japan, Co. Ltd., Kanagawa, Japan). The protein concentration of the supernatants was determined with BCA reagent using bovine serum albumin as a standard and cps/μg protein was calculated.

GFP expression was analyzed by fluorescence microscopy and flow cytometer. For fluorescence microscopy,

RESEARCH ARTICLE

at the end of the incubation, the dishes were washed 3 times with 1 mL of PBS and fixed with 10% formaldehyde PBS at room temperature for 20 min, and washed three times with PBS. Then, the cells were coated with Aqua Poly/Mount (Poly science, Warrington, PA) to prevent fading and covered with coverslips. The fixed cells were observed with an ECLIPSE TS100/100-F for Epi-fluorescence Observations. The contrast level and brightness of the images were adjusted.

2.8. Data Analysis

Significant differences in the mean values were evaluated using Student's unpaired *t*-test. A *p*-value of less than 0.05 was considered significant.

3. RESULTS AND DISCUSSION

3.1. Characterization and Transfection Efficiency of Arg10-PEG-BDB

In order to determine the CMC of Arg10-PEG-BDB in water, we monitored fluorescence intensity as we added different concentrations of Arg10-PEG-BDB into an aqueous dispersion of pyrene. The CMC value of Arg10-PEG-BDB was 20.9 μM or 83.6 μg/mL at room temperature (Fig. 2).

Particle size and the zeta-potential of Arg10-PEG-BDB (25 μM)/DNA (N/P = 42.5/1) complex were about 1500 nm and 42.7 mV, respectively (Table I). The zeta-potential of the complex (5 μM, N/P = 8.5/1, 27.1 mV) decreased by about 10 mV compared with that of Arg10-PEG-BDB micelles (38.0 mV) due to the negative charge of DNA.

We examined the influence of the concentration of Arg10-PEG-BDB on transfection efficiency by luciferase activity. The highest transfection efficiency was observed at the concentration of 5 μM of Arg10-PEG-BDB (N/P = 8.5/1), which is significantly (1.5-fold) higher than that of

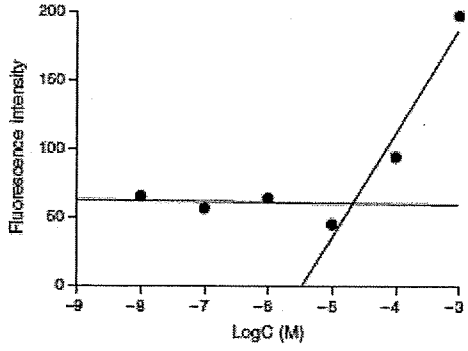

Fig. 2. CMC measurements of Arg10-PEG-BDB by fluorescence probe method using pyrene.

Table I. Particle size and zeta-potential of Arg10-PEG-BDB complexed with or without DNA.

Lipid concentration and complex[a]	N/P	Size (nm)	Zeta-potential (mV)
Arg10-PEG-BDB (25 μM)		N.D.[b]	+38.0
Arg10-PEG-BDB (5 μM)/DNA	8.5/1	N.D.[b]	+27.1
Arg10-PEG-BDB (25 μM)/DNA	42.5/1	~1500	+42.7

[a]Complex with 2 μg of DNA.
[b]N.D., not detected by dynamic light scattering method.

25 μM (Fig. 3(A)), superficially suggesting that micelle formation is not necessary for high transfection efficiency. To examine the distribution of transfection in cells, we observed the transfection efficiency of Arg10-PEG-BDB with the plasmid pEGFP-C1 using flow cytometry and fluorescence microscopy. 5 μM of Arg10-PEG-BDB showed about 7-fold higher transfection efficiencies than 25 μM (Fig. 3(B)). A significantly higher level of GFP protein was observed in the cells treated with 5 μM of Arg10-PEG-BDB than 25 μM, corresponding to the results of luciferase expression (Fig. 3(C)).

The higher concentration of Arg10-PEG-BDB/DNA could not be used because cytotoxicity was increased with an increase of lipid concentration.[12] The cytotoxicity of 5 μM of Arg10-PEG-BDB/DNA, therefore, was lower than that of 25 μM. To clarify the underlying mechanisms that dictated the remarkable differences between 5 and 25 μM in lipid-mediated transfection efficiency, the properties of lipid complexes with DNA were investigated.

3.2. Investigation of the Interaction of Arg10-PEG-BDB with DNA by FIDA

To examine the interaction of Arg10-PEG-BDB with DNA, Arg10-PEG-BDB and 2 μg rhodamine-DNA was mixed and characterized using FIDA with a MF20 microplate reader (Olympus Corp. Tokyo, Japan).[9] A theoretical probability distribution of photon count numbers is fitted against the obtained histogram, yielding specific brightness values Q and concentrations C for all different species in a sample. Decreased C value and increased Q value were observed at the concentration of 1~5 μM of Arg10-PEG-BDB, suggesting that more DNA bound to Arg10-PEG-BDB in this concentration range (Figs. 4(A, B)). The data showed that the interaction of 5 μM of Arg10-PEG-BDB with DNA (N/P = 8.5/1) was stronger than that of 25 μM (N/P = 42.5/1). DNA might help the self-aggregation of Arg10-PEG-BDB even at low concentrations of lipid. This effect may be reflected in the highest transfection efficiency at the 5 μM concentration of Arg10-PEG-BDB to 2 μg DNA. To examine whether this difference of interaction of lipid with DNA in complexes by the concentration of lipid correlated with the differences in structural feature, the complexes were further characterized by electron microscopy.

RESEARCH ARTICLE

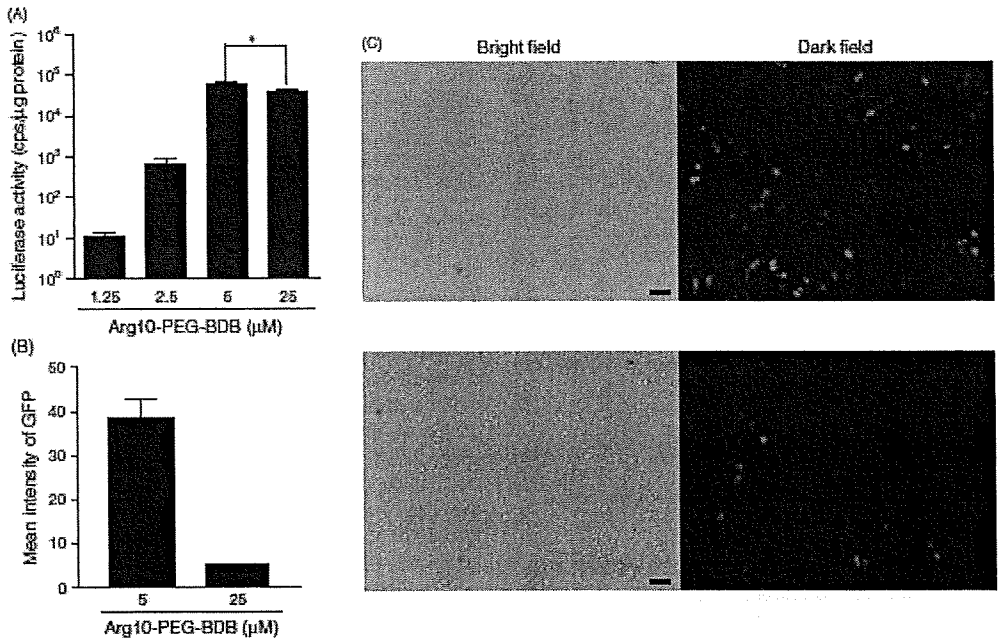

Fig. 3. Influence of the concentration of Arg10-PEG-BDB complexed with DNA on transfection efficiency. Arg10-PEG-BDB/DNA complexes (prepared by mixing 2 μg of pCMV-luc or pEGFP-C1 with various concentrations of Arg10-PEG-BDB) were diluted with serum-free DMEM to a final volume of 1 mL. After incubation for 3 h at 37 °C in serum-free DMEM, DMEM (1 mL) containing 10% FBS was added, and the cells were further incubated for 21 h. (A) Luciferase activity of various concentrations of Arg10-PEG-BDB. (B) GFP expression of 5 or 25 μM of Arg10-PEG-BDB. Each value is the mean ± S.D. of three separate determinations. (C) Analysis of GFP expression by fluorescence microscopy (magnification ×100). 5 μM of Arg10-PEG-BDB (top) and 25 μM of Arg10-PEG-BDB (bottom) are shown. Scale bar = 50 μm.

3.3. The Morphology of Arg10-PEG-BDB/DNA Complexes Determined by Electron Microscopy and Microscopy

To reveal the nanostructure of Arg10-PEG-BDB/DNA complexes under various concentrations of lipid, we observed the Arg10-PEG-BDB/DNA complex using phase contrast cryo-TEM. Free DNA papered was observed as open circular one (data not shown). To observe the lipid structure, two higher concentrations of Arg10-PEG-BDB were examined at the same (N/P) ratio as the transfection experiments. Micellar structures with several nm sizes were observed at 1.25 mM of Arg10-PEG-BDB above CMC (Fig. 5(A)). In Arg10-PEG-BDB/DNA complex (N/P = 8.5/1), a net-like structure was observed in which DNA was involved (Fig. 5(B)). These net-like structures may contribute to high transfection efficiency, but the particle size of Arg10-PEG-BDB (5 μM, 0.25 mM)/DNA (N/P = 8.5/1) in water was not detected by dynamic light scattering method. Surprisingly, in the Arg10-PEG-BDB/DNA complex (N/P = 42.5/1), heterogeneous nanostructures were observed. Other than net-like structures, large fibrous nanostructures were visible (Fig. 5(C)). Their particle size of Arg10-PEG-BDB (1.25 mM)/DNA (N/P = 42.5/1) in water was about 1.5 μm by dynamic light scattering method. In both cases we can clearly see DNA molecules around the edge of the net-like structures.

At a lower magnification, we observed the structure at the same condition as the transfection by the microscopy. Cells were exposed for 1 h to the 5 or 25 μM of Arg10-PEG-BDB/DNA complex in the absence of serum. Next, the unfixed cells were visualized by microscopy. It was hardly observed in 5 μM of Arg10-PEG-BDB/DNA, but a large aggregation was observed in 25 μM (Figs. 6(A, B)). The large aggregation of 25 μM of Arg10-PEG-BDB/DNA, therefore, might inhibit the cell internalization or the release of DNA from endosomes into cytoplasm.

Increase of lipid concentration appeared to tend to convert from net-like structures into a large fibrous one. Previously, we reported that the structure of PEG-BDB became fiber with the increase of lipid concentration.[20] At higher concentration of Arg10-PEG-BDB, DNA might induce the fibrous nanostructure by partial neutralization of Arg10-PEG-BDB, suggesting that DNA may modulate the net-like structure and fibrous nanostructure of Arg10-PEG-BDB. The former reflected a stronger interaction between DNA and lipid than the latter. To further investigate effect of the difference of nanostructures of complexes

RESEARCH ARTICLE

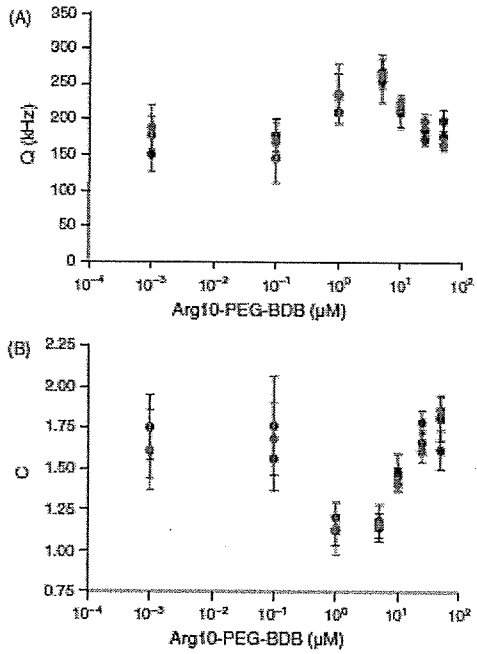

Fig. 4. Fluorescence intensity distribution analysis (FIDA) of Arg10-PEG-BDB and 2 μg rhodamine-DNA complex. (A) Brightness per complex; Q value. (B) Fluorescent DNA number; C value. Each value is the mean ± S.D. of three separate determinations.

on transfection efficiency, cellular uptake mechanism was subsequently examined.

3.4. Cellular Uptake Mechanism

The difference of nanostructures of complexes may cause difference in the ability to deliver DNA into HeLa cells. At first, to examine the association of Arg10-PEG-BDB/DNA complex with cells, we assayed the cell internalization of 5 or 25 μM of the Arg10-PEG-BDB/DNA 3 h after transfection with serum by flow cytometry (Fig. 7(A)). To remove bind Arg10-PEG-BDB/DNA on the surface of plasma membrane, we washed the cells with PBS and treated them with trypsin.[21] Associated amount of 5 or 25 μM of Arg10-PEG-BDB/DNA with the cells was almost same, indicated that both concentrations of Arg10-PEG-BDB were able to carry similar amount of rhodamine-DNA into cells.

The cellular uptake pathway is reported to be different depending on the density of octaarginine (Arg8) in liposome containing Arg8.[22] Hence, there is a possibility that the cellular uptake mechanism might change depending on the concentration of Arg10-PEG-BDB. The translocation of Tat and Arg8 peptide are suggested to occur through macropinocytosis which is dependent on lipidic

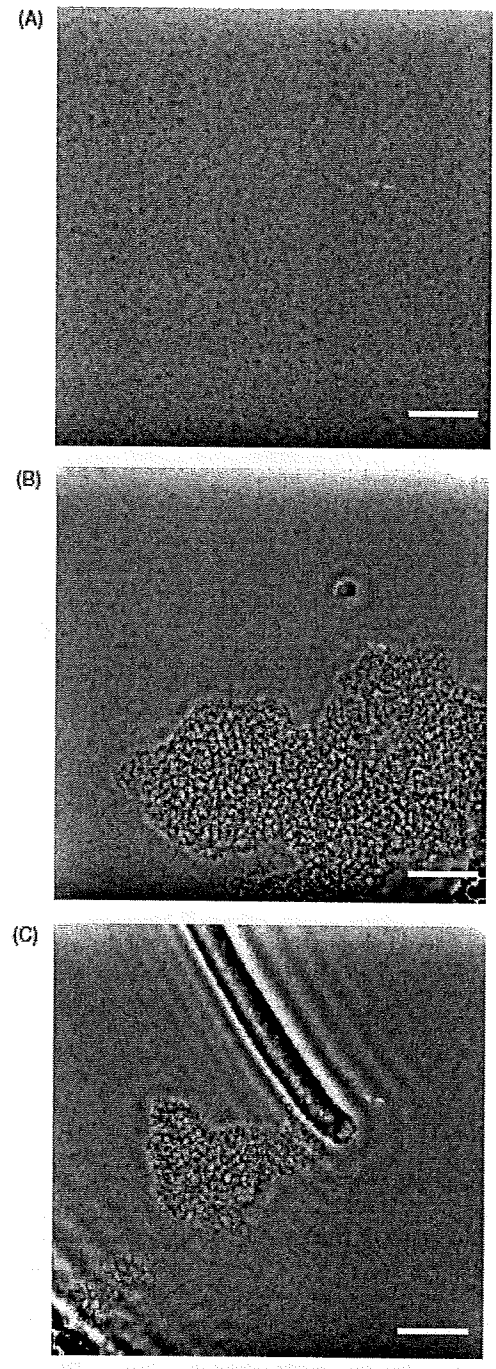

Fig. 5. Phase contrast cryo-TEM analysis of the complex structure of Arg10-PEG-BDB and DNA. (A) 1.25 mM of Arg10-PEG-BDB. (B) 0.25 mM of Arg10-PEG-BDB/DNA (N/P = 8.5/1). (C) 1.25 mM of Arg10-PEG-BDB/DNA (N/P = 42.5/1). Scale bar = 100 nm.

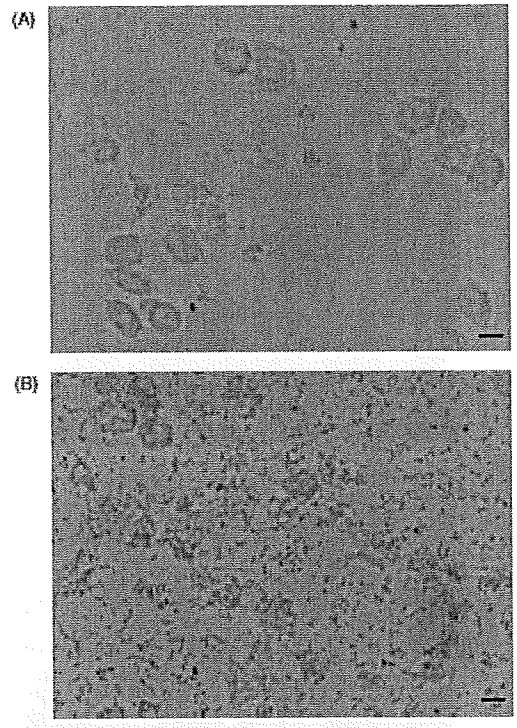

Fig. 6. Microscopic analysis of the Arg10-PEG-BDB/DNA complex incubated with the cells for 1 h at 37 °C in serum-free DMEM. The unfixed cells were observed with a microscope. (A) 5 μM of Arg10-PEG-BDB/DNA (N/P = 8.5/1). (B) 25 μM of Arg10-PEG-BDB/DNA (N/P = 42.5/1). Scale bar = 20 μm.

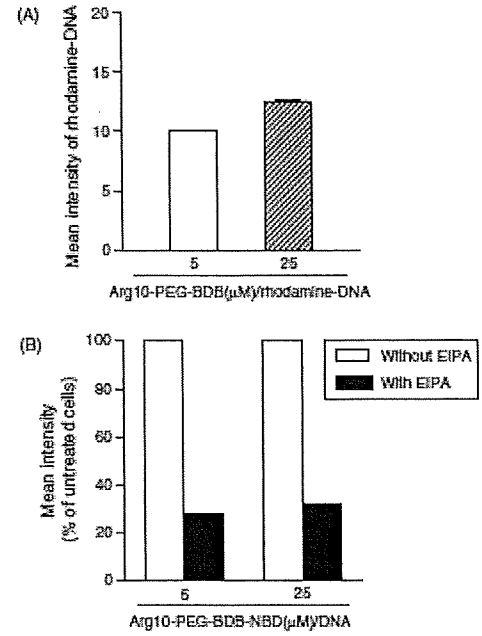

Fig. 7. (A) Cellular uptake of 5 or 25 μM of Arg10-PEG-BDB/rhodamine-DNA incubated for 3 h at 37 °C. The cells were treated with trypsin before flow cytometry. (B) Effect of EIPA on their cellular uptake. Cells were pretreated with EIPA (50 μM) at 37 °C for 30 min. Medium was replaced with fresh medium containing 5 or 25 μM Arg10-PEG-BDB-NBD/2 μg DNA. Cells were incubated for 1 h at 37 °C in serum DMEM containing EIPA (50 μM). Each value is the mean ± S.D. of three separate determinations.

microdomains.[23,24] Macropinocytosis is a kind of endocytosis as a cellular uptake pathway.[25] Macropinosomes are formed by actin-driven ruffling of the plasma membrane, followed by folding and pinching off of irregular-sized vesicles.[26] Macropinocytosis is inhibited by 5-(*N*-ethyl-*N*-isopropyl) amiloride (EIPA), which inhibits Na^+/H^+ exchange protein.[23] To examine the internalization mechanism of 5 and 25 μM Arg10-PEG-BDB/DNA (N/P = 8.5/1 and 42.5/1), we investigated the effect of EIPA on the cellular uptake of complexes, using Arg10-PEG-BDB-NBD (Fig. 7(B)). Arg10-PEG-BDB-NBD (5 and 25 μM)/DNA showed about 70% lower internalization efficiency at 50 μM of EIPA than in its absence. This finding suggests that 5 and 25 μM of Arg10-PEG-BDB/DNA were taken up via a macropinocytosis pathway although their structures were different (Figs. 5(B, C)). DNA may be released easily in the cytoplasm because it is reported that macropinosomes are leaky.[27] The large fibrous nanostructure, therefore, might inhibit the release of DNA from macropinosomes into cytoplasm. At the present research technique, it is difficult to examine it further since the research of CPP should be observed at unfixed cells.

4. CONCLUSIONS

Arg10-PEG-BDB at the concentration below CMC showed higher transfection efficiency in HeLa cells than that above CMC. In Arg10-PEG-BDB/DNA complex below CMC, a net-like structure was observed. On the other hand, in the Arg10-PEG-BDB/DNA complex above CMC, heterogenous structures composed of net-like and large fibrous structures were observed. It is very important that plasmid DNA is able to help Arg10-PEG-BDB to form supramolecular structures. DNA-assisted Arg10-PEG-BDB nanostructure formation may result in concentration-dependent transfection efficiency.

Acknowledgments: This project was supported in part by a grant from the Promotion and Mutual Aid Corporation for Private Schools of Japan and by a Grant-in-Aid for Scientific Research from the Ministry of Education, Culture, Sports, Science, and Technology of Japan. This study was supported in part by the Ministry of Education, Culture, Sports, Science and Technology, Japan, and by the Open Research Center Project.

RESEARCH ARTICLE

References and Notes

1. T. Niidome and L. Huang, *Gene Ther.* 9, 1647 (2002).
2. E. Marshall, *Science* 286, 2244 (1999).
3. P. L. Felgner, T. R. Gadek, M. Holm, R. Roman, H. W. Chan, M. Wenz, J. P. Northrop, G. M. Ringold, and M. Danielsen, *Proc. Natl. Acad. Sci. U.S.A.* 84, 7413 (1987).
4. T. B. Potocky, J. Silvius, A. K. Menon, and S. H. Gellman, *Chembiochem* 8, 917 (2007).
5. D. J. Mitchell, D. T. Kim, L. Steinman, C. G. Fathman, and J. B. Rothbard, *J. Pept. Res.* 56, 318 (2000).
6. P. A. Wender, D. J. Mitchell, K. Pattabiraman, E. T. Pelkey, L. Steinman, and J. B. Rothbard, *Proc. Natl. Acad. Sci. U.S.A.* 97, 13003 (2000).
7. S. Futaki, T. Suzuki, W. Ohashi, T. Yagami, S. Tanaka, K. Ueda, and Y. Sugiura, *J. Biol. Chem.* 276, 5836 (2001).
8. S. Futaki, W. Ohashi, T. Suzuki, M. Niwa, S. Tanaka, K. Ueda, H. Harashima, and Y. Sugiura, *Bioconjug. Chem.* 12, 1005 (2001).
9. M. Furuhata, H. Kawakami, K. Toma, Y. Hattori, and Y. Maitani, *Bioconjug. Chem.* 17, 935 (2006).
10. K. Kogure, R. Moriguchi, K. Sasaki, M. Ueno, S. Futaki, and H. Harashima, *J. Control. Release* 98, 317 (2004).
11. W. J. Kim, L. V. Christensen, S. Jo, J. W. Yockman, J. H. Jeong, Y. H. Kim, and S. W. Kim, *Mol. Ther.* 14, 343 (2006).
12. M. Furuhata, H. Kawakami, K. Toma, Y. Hattori, and Y. Maitani, *Int. J. Pharm.* 316, 109 (2006).
13. M. X. Tang and F. C. Szoka, *Gene Ther.* 4, 823 (1997).
14. I. Smisterova, A. Wagenaar, M. C. A. Stuart, E. Polushkin, G. ten Brinke, R. Hulst, J. B. F. N. Engberts, and D. Hoekstra, *J. Biol. Chem.* 276, 47615 (2001).
15. B. Pitard, O. Aguerre, M. Airiau, A. M. Lachages, T. Boukhnikachvili, G. Byk, C. Dubertret, C. Herviou, D. Scherman, J. F. Mayaux, and J. Crouzet, *Proc. Natl. Acad. Sci. U.S.A.* 94, 14412 (1997).
16. S. Igarashi, Y. Hattori, and Y. Maitani, *J. Control. Release* 112, 362 (2006).
17. C. L. Zhao, M. A. Winnik, G. Riess, and M. D. Croucher, *Langmuir* 6, 514 (1990).
18. R. Danev and K. Nagayama, *Ultramicroscopy* 88, 243 (2001).
19. K. Nagayama, *Adv. Imag. Elect. Phys.* 138, 69 (2005).
20. T. Yoshitomi, S. Yabuki, H. Kawakami, R. Sato, K. Toma, M. Furuhata, and Y. Maitani, *Colloids. Surf. A Physicochem. Eng. Asp.* 284–285, 276 (2006).
21. J. P. Richard, K. Melikov, E. Vives, C. Ramos, B. Verbeure, M. J. Gait, L. V. Chernomordik, and B. Lebleu, *J. Biol. Chem.* 278, 585 (2003).
22. I. Khalil, K. Kogure, S. Futaki, and H. Harashima, *J. Biol. Chem.* 281, 3544 (2006).
23. J. S. Wadia, R. V. Stan, and S. F. Dowdy, *Nat. Med.* 10, 310 (2004).
24. I. Nakase, M. Niwa, T. Takeuchi, K. Sonomura, N. Kawabata, Y. Koike, M. Takehashi, S. Tanaka, K. Ueda, J. C. Simpson, A. T. Jones, Y. Sugiura, and S. Futaki, *Mol. Ther.* 10, 1011 (2004).
25. S. D. Conner and S. L. Schmid, *Nature* 422, 37 (2003).
26. S. Grimmer, B. van Deurs, and K. Sandvig, *J. Cell Sci.* 115, 2953 (2002).
27. O. Meier, K. Boucke, S. V. Hammer, S. Keller, R. P. Stidwill, S. Hemmi, and U. F. Greber, *J. Cell Biol.* 158, 1119 (2002).

Received: 3 October 2007. Accepted: 23 October 2007.

RESEARCH ARTICLE